MAGNETIC PROPERTIES OF PERMALLOY THIN FILM EDGES

B. A. Belyaev,[1,2] **N. M. Boev,**[1,2] **A. V. Izotov,**[1,2] **G. V. Skomorokhov,**[1] **and P. N. Solovev**[1,2]   UDC 537.622

The paper presents the results of ferromagnetic resonance (FMR) spectrometry of magnetic properties of nanocrystalline thin films obtained by magnetron sputtering of permalloy targets of various composition (Ni_xFe_{1-x}*, x = 0.6–0.85). The behavior of the main magnetic properties of the thin film edges is analyzed. Near the film edges, not only the fluctuation of the uniaxial magnetic anisotropy field is observed, but also a drastic widening of the FMR line and the decrease in the effective saturation magnetization.*

Keywords: magnetic thin film, ferromagnetic resonance, edge effects, magnetic anisotropy.

INTRODUCTION

In recent years, nanocrystalline thin magnetic films have attracted much attention for researchers owing to the rapidly increasing demand for magnetic materials possessing high magnetic susceptibility [1]. In particular, nanocrystalline thin magnetic films with high magnetic susceptibility in the microwave range have important radio engineering applications, for example, the development of magnetic field sensors [2, 3], gradiometers [4], phase converters, and frequency multipliers [5]. The unique soft magnetic properties of nanocrystalline magnetic films are provided by their microstructure. In the case of randomly oriented crystal grains with the size lower than the exchange-interaction correlation radius, the exchange energy dominates the energy of magnetocrystalline anisotropy and levels the distribution of magnetic anisotropy axes of the crystal grains, resulting in a very low coercive force [6] and high magnetic susceptibility over the film [7–9]. However, there are factors that lead to spatial variations in the magnetic properties of the film area. An increase in the magnetic anisotropy dispersion, saturation magnetization, and FMR line width significantly reduces the magnetic susceptibility and increases the magnetic noise of the thin film, which will have a negative impact on the performance of devices utilizing such films as active media. In our previous research [10] we report that in a weak magnetic field sensor with the film used as a sensitive element, the conversion ratio monotonically decreases with increasing amplitude and angular dispersion of the magnetic anisotropy field, the angular dispersion providing a stronger effect. Experience shows that the most irregular distribution of magnetic properties over thin magnetic films is usually observed at their edges. Edge effects may be of different nature. When magnetization is not parallel to the film edge, inhomogeneous demagnetizing fields occur nearby, providing, in particular, the conditions for inhomogeneous oscillations of magnetization at the film edges [11]. At the same time, the asymmetric distortion at the film edges enables the formation of mechanical stress gradients [12], which affect the film magnetic properties through magnetostriction [13]. It is important to note that stress gradients can also lead to the formation of the unidirectional magnetic anisotropy [14]. Moreover, the conditions of the film growth near the edges often differ from that of its center [15], which may lead to the formation of an inhomogeneous microstructure near the film edges.

In our recent research [16], we used different methods to measure the distribution of magnetic properties over

---

[1]Kirensky Institute of Physics of the Siberian Branch of the Russian Academy of Sciences, Krasnoyarsk, Russia, e-mail: belyaev@iph.krasn.ru; tornadobak@mail.ru; psolovev@iph.krasn.ru; [2]Siberian Federal University, Krasnoyarsk, Russia, e-mail: nik88@inbox.ru; iztv@mail.ru.

the nanocrystalline thin permalloy films. We studied the nature of the parameter distribution of the uniaxial magnetic anisotropy near the film edges.

This work presents the results of ferromagnetic resonance (FMR) spectrometry of magnetic parameters of NiFe thin films that are prepared by magnetron sputtering of a permalloy target of various composition. The behavior of the main magnetic properties of the film edges are considered in detail.

MATERIALS AND METHODS

Nanocrystalline thin magnetic films were prepared by magnetron sputtering of low-impurity (0.05 wt.%) targets of the following five compositions (in wt.%): $Ni_{60}Fe_{40}$, $Ni_{70}Fe_{30}$, $Ni_{75}Fe_{25}$, $Ni_{80}Fe_{20}$, and $Ni_{85}Fe_{15}$. The targets represented 2 mm thick discs with a diameter of 55 mm. In all, 25 NiFe films were obtained (five films from each disc). The films were deposited onto $12\times12\times0.5$ mm silica glass substrates with the surface roughness less than 1 nm. The substrates were preliminary coated with a 500-nm-thick SiO layer and then placed on a copper holder having 10×10 mm windows. The distance between the target and the substrate holder was 170 mm. The magnetron power density was constant (11 W/cm^2), which provided the deposition rate of 0.25 nm/s. The base pressure in the chamber and argon gas pressure were $3\cdot10^{-4}$ and $2\cdot10^{-1}$ Pa, respectively. Each magnetic film was ~60 nm thick. During the deposition process, the substrate was kept at a constant temperature of 200°C. The external magnetic field of 200 Oe was applied to the film plane. For all but one of the magnetic films, the external magnetic field was parallel to one substrate edge (Y axis). One magnetic film was prepared by $Ni_{80}Fe_{20}$ target sputtering using a circular mask with a 10 mm diameter.

The chemical composition of the sputter-deposited films was analyzed by X-ray fluorescence spectrometry. It was found that the difference between the film and target compositions was less than 1.5 wt.%. The film microstructure analyzed on a transmission electron microscope (TEM), was nanocrystalline, with grain size ranging between 6–14 nm. The X-ray diffraction patterns of the sputter-deposited films indicated to randomly oriented crystal grains. In addition, cross-section TEM images of the films showed their columnar microstructure, with the column width of about 10 nm. It should be noted that the columnar microstructure was typical for thin films produced at substrate temperatures lower than the melting point of the metal deposited [17, 18].

The magnetic properties of the sputter-deposited films were studied using an FMR scanning-spectrometer equipped with a microstrip resonator sensor with slotted ground plane mounted to the dielectric substrate near the antinode of the high-frequency magnetic field [19]. The slot of about ~1 mm determined the measurement localization. The main advantage of this spectrometer was a high sensitivity even at a relatively low (2.3 GHz) pumping frequency because of the high duty cycle of the miniature resonator. The effective saturation magnetization and the uniaxial magnetic anisotropy parameters of each local place were determined by the angular dependences of the resonance field *via* a selection of the theoretical model parameters of a single domain film to provide agreement between theoretical calculations and experimental data [20, 21]. Measurements were conducted for the whole film area at a step size of 1 mm.

RESULTS AND DISCUSSION

The distribution of magnetic properties over the film areas is measured with an FMR scanning-spectrometer. Figure 1 presents the FMR images of two $Ni_{80}Fe_{20}$ films. The films are sputtered through the mask with a square and circular window, respectively. According to Fig. 1, a relatively high homogeneity of the distribution of magnetic properties in the film center is severely affected at its edges. A strong fluctuation of the uniaxial magnetic anisotropy field H_a is observed, while the effective saturation magnetization M_s notably lowers. Moreover, the FMR line width ΔH increases sharply at the film edges. In Fig. 1*a*, at the opposite film side, along which the external magnetic field H_{ext} is directed during deposition, the uniaxial magnetic anisotropy field H_a is approximately 25% larger than that at the center. At the film edges of the other opposite sides, the uniaxial magnetic anisotropy field is about as small as in the first case. The easy-axis distribution (white line marks in Fig. 1) is not well-defined near the film edges, and the easy-axis
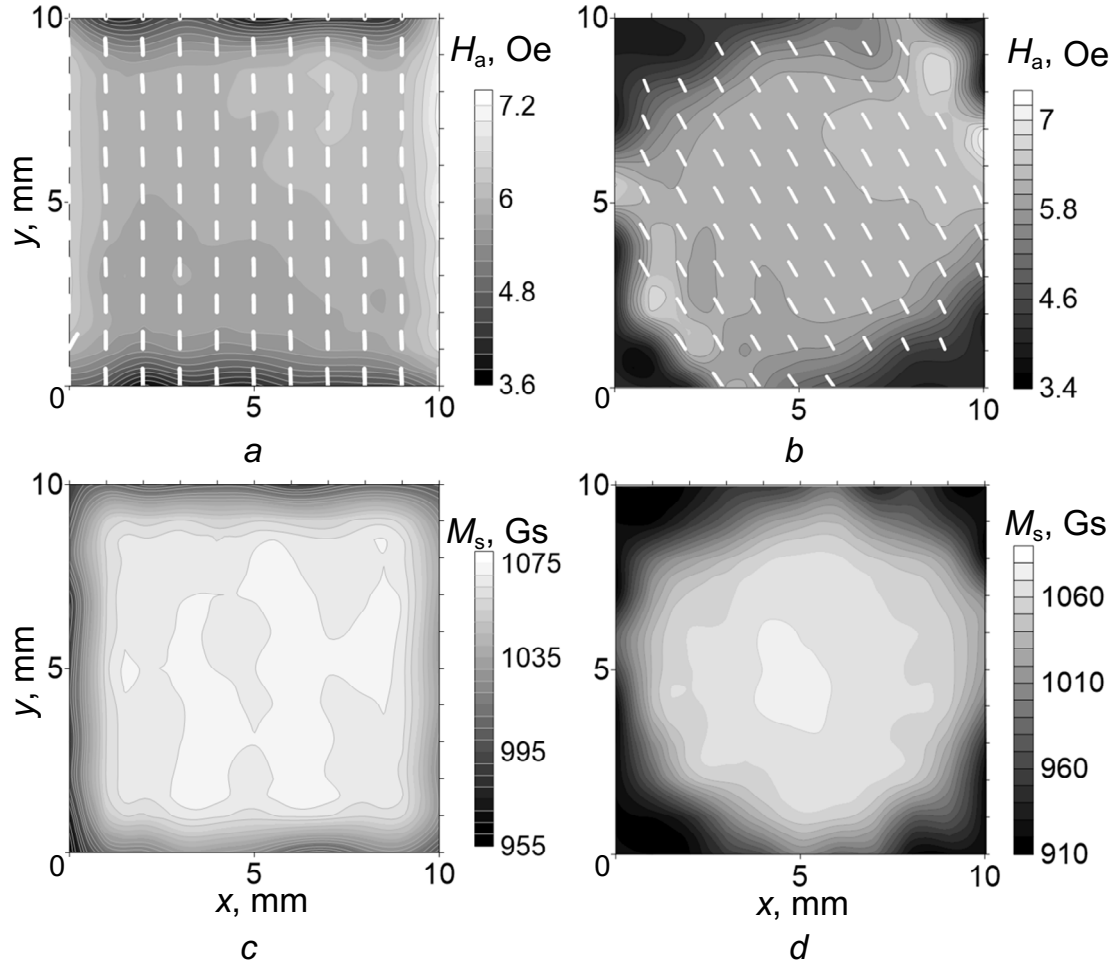
Fig. 1. FMR images of two $Ni_{80}Fe_{20}$ films with magnetic property distribution: *a*, *c* – square film, *b*, *d* – circular film. H_a – uniaxial magnetic anisotropy field, M_s – effective saturation magnetization. White line marks indicate the easy-axis distribution.

orientation matches the magnetic field direction. Figure 1*b* shows a similar pattern for the film deposited through the mask with a circular window. At the film edges one can see a decrease in the effective saturation magnetization M_s, whereas the anisotropy field is maximum near the film edges which are closer to the magnetic field direction. However, since this film is circular, it has only two points at the opposite sides with edges strictly parallel or normal to the magnetic field. The easy axis of the circular film is directed along the magnetic field, which in turn is directed at an angle of 120 degrees relative to the *X* axis. The angular distribution of easy axes will be discussed below.

The obtained results show that magnetic anisotropy in all the square films is almost symmetrical at the opposite edges. As can be seen from Fig. 2*a*, the positive fluctuation of the uniaxial magnetic anisotropy field H_a at the film edges from the average value is slightly greater than the negative. Here, S_H is defined by the ratio between H_a absolute deviations along *X* and *Y* axes at the film edges. The S_H value is low-dependent on the target composition, and the positive H_a deviation along the *Y* axis is 25% larger than the negative one along the *X* axis.

As is shown in Fig. 1, the film edges significantly contribute to the total dispersion of magnetic characteristics over the film area. In Fig. 2*b*, the dependence is obtained for the root-mean-square (RMS) fluctuation of the anisotropy
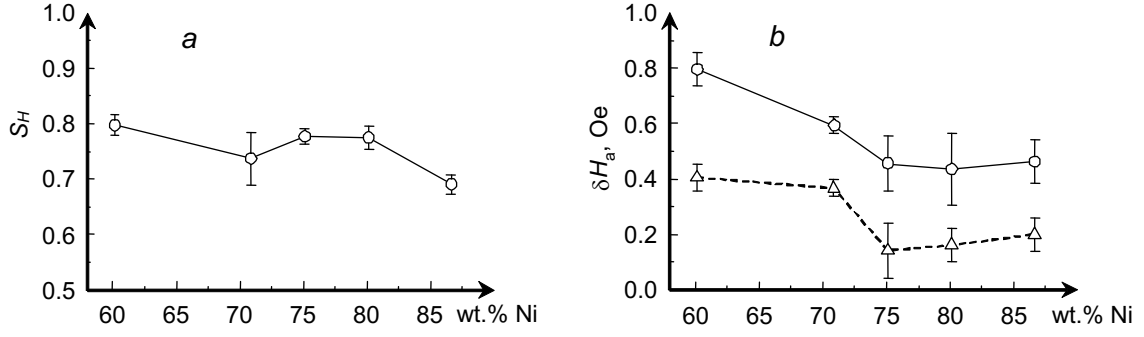
Fig. 2. Absolute fluctuations of the uniaxial magnetic anisotropy field H_a at the adjacent film edges S_H (*a*) and the RMS fluctuation of the anisotropy field δH_a (*b*) depending on the target composition. Circles and triangles indicate fluctuations over the whole target area and 1 mm away from the edge, respectively.

field $\delta H_a = \sqrt{(1/n)\sum_{i=1}^{n}(H_a^i - <H_a>)^2}$ and the target composition. $<H_a>$ is the mean value of the uniaxial magnetic anisotropy field; H_a^i is the anisotropy field of the *i*-th local area of the film, *n* is the number of measurement points. Figure 2*b* presents the RMS fluctuation of the anisotropy field δH_a both over the whole target area ($n = 100$) and 1 mm away from the edge ($n = 64$). One can see that the RMS fluctuation of the anisotropy field δH_a decreases with increasing nickel content in permalloy, reaches a minimum for the $Ni_{80}Fe_{20}$ composition, and then starts to grow. This is probably due to the dependence between constant magnetostriction and the permalloy target composition. The constant magnetostriction for $Ni_{80}Fe_{20}$ tends to zero, which leads to leveling of the dispersion mechanisms associated with mechanical stresses in the film. For all compositions, the fluctuation of the anisotropy field over the area 1 mm away from the edge is, however, about 2 times less than that over the whole area.

As can be expected, the measurement results show that the magnetic anisotropy field strongly depends on the target composition. It is therefore interesting to investigate not only the average distribution of magnetic anisotropy $<H_f>$ in each specimen without edges (1 mm margin), but also the edge effect contribution as a function of the nickel content in the permalloy target. The contribution of the edge effects is determined by the mean value of $<H_e>$, which is the absolute difference between the mean values of H_a for each pair of opposite edges and $<H_f>$. The latter can be approximated as the averaged uniaxial magnetic anisotropy field induced by the magnetic field, while $<H_e>$ value – as the averaged effective magnetic anisotropy field near the film edges. The obtained dependencies are presented on Fig. 3*a*. The mean value of the magnetic anisotropy field $<H_f>$ linearly decreases with the nickel content increasing from 60 to 86 wt.%. This dependence reproduces the well-known results concerning the NiFe films, which are explained by the theory of ordering atomic pairs exposed to a magnetic field during the deposition process [22]. The mean value of $<H_e>$ also linearly depends on the target composition and decreases from 2.17 Oe for 60 wt.% Ni to 1.3 Oe for 86 wt.% Ni. In Fig. 3*b*, the dependence is shown for the ratio $<H_e>/<H_f>$ and the target composition. With increasing nickel content in permalloy, this ratio increases, the dependence being nonlinear. It is interesting to consider two assumptions. Let the averaged magnetic anisotropy fields $<H_f>$ and $<H_e>$ equally depend on the target composition, and let $<H_e>$ does not depend on it. These two cases are described by the solid and dotted lines in Fig. 3*b*. One can see that the experimental dependence is in the intermediate position between the two approximations. This suggests that different mechanisms are responsible for the formation of magnetic anisotropy fields $<H_f>$ and $<H_e>$.

According to [16], the observed behavior of the anisotropy fields can be explained by assuming that there is a mechanism that additionally contributes to the uniaxial magnetic anisotropy with the easy axis parallel to the film edges. In the case of two formation mechanisms, the resulting anisotropy field equals the sum of two anisotropy fields (if easy axes are parallel) or their difference (if easy axes are perpendicular), and the resulting easy axis is directed along the easy axis of the larger anisotropy. This exactly matches the H_a behavior shown in Fig. 1*a*. However, in
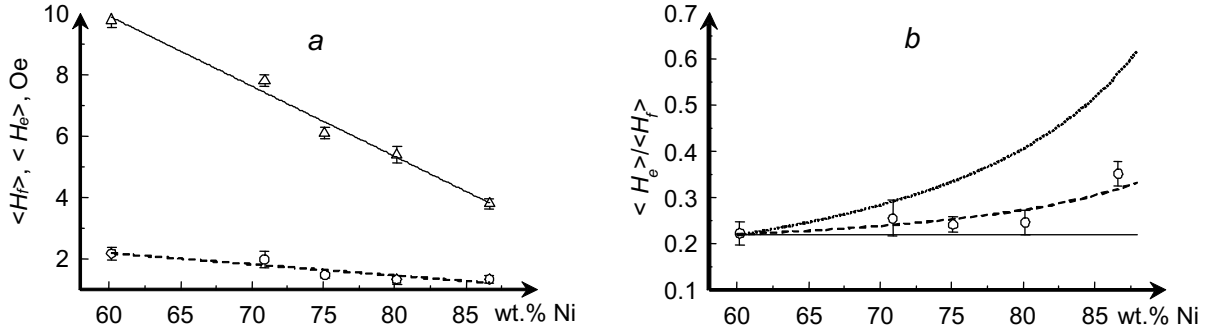
Fig. 3. Dependencies of averaged magnetic anisotropy fields $<H_f>$ (triangles) and $<H_e>$ (circles) on Ni concentration in permalloy. Lines indicates linear approximations (*a*). Dependence between $<H_e>/<H_f>$ ratio and the target composition. Circles denote experimental data, dashed line with circles denotes approximated experimental data, solid line indicates the similar dependence of $<H_f>$ and $<H_e>$ on the target composition, and dotted line shows the $<H_e>$ independence on the target composition (*b*).
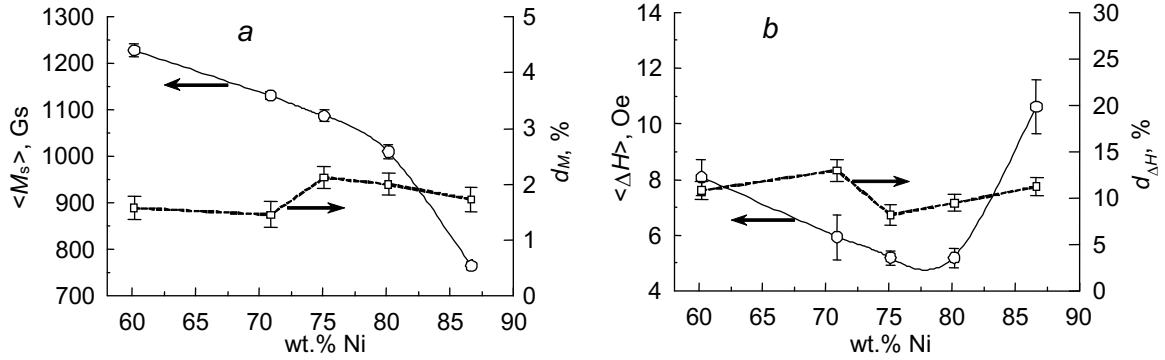
Fig. 4. Dependencies of the average effective saturation magnetization $<M_s>$ (*a*) and average FMR line width $<\Delta H>$ (*b*) on the target composition (circles) and on the relative change of these parameters at the film edges d_M and $d_{\Delta H}$ (squares).

general case of the arbitrary orientation of the two easy axes, the easy axis of the resulting uniaxial anisotropy should be in an intermediate position between them. This is shown in Fig. 1*b* for the circular film. Actually, at the circular film edges parallel to H_{ext} field, the maximum H_a should be observed, whereas at the local film areas, with edges normal to the H_{ext} field, the H_a field should be minimum, the easy axis being parallel to the H_{ext}, as observed in the experiment. At the same time, according to [16], if the angle between the film edge and H_{ext} field is 45 degrees, the resulting anisotropy field is approximately equal to $<H_f>$ field, and its easy-axis orientation deviates from H_{ext} field by several degrees. The obtained parameters of the circular film anisotropy confirm this conclusion, *i.e.* the maximum deviation (~7 degrees) of the easy axis from the H_{ext} field direction is observed near the film edges composing an angle of ~45 degrees with the field H_{ext}.

It was highlighted that not only the behavior of magnetic anisotropy parameters is specific at the film edges, but also the nature of the distribution of effective saturation magnetization M_s and the FMR line width ΔH. At the film edges, the saturation magnetization M_s slightly decreases relative to the film center, while the FMR line substantially widens. The dependences of the effective saturation magnetization $<M_s>$ and the averaged FMR line width $<\Delta H>$ on the area-mean film composition are given in Fig. 4. The dependencies of d_M and $d_{\Delta H}$ values on the film composition are

20

also shown. Here d_M value denotes a relative decrease in M_s at the film edges, whereas $d_{\Delta H}$ value describes a relative increase in $d_{\Delta H}$ at the film edges. The value of $<M_s>$ decreases monotonically with increasing Ni content, that is in good agreement with the data for the bulk permalloy specimens [23]. As can be seen from Fig. 4, the value of d_M does not depend on the target composition, and on average, for all the 25 specimens, the decrease in the saturation magnetization M_s at the film edges is ~1.8% as compared to the film center. With growing nickel content in permalloy, the averaged FMR line width $<\Delta H>$ decreases down to ~75–80 wt.% Ni and then drastically increases. The behavior of the $<\Delta H>$ value is similar to that of the anisotropy field δH_a (see Fig. 2*b*), which is probably caused by the same reasons. It is interesting to note that the relative increase in the FMR line width at the film edges $d_{\Delta H}$ does not depend on the target composition (Fig. 4*b*) and is 10.5% on average.

CONCLUSIONS

Ferromagnetic resonance spectrometry allowed investigating the distribution of magnetic properties over the area of nanocrystalline thin films obtained by magnetron sputtering of permalloy targets. The analysis of the main magnetic properties at the film edges showed a strong fluctuation of the uniaxial magnetic anisotropy field, a sharp growth in the FMR line width and a small decrease in the effective saturation magnetization relative to the film center. The additional effective contribution to the uniaxial anisotropy was observed at the film edges, and the formation mechanisms of this additional contribution and the uniaxial anisotropy at the film center were of different nature.

The important practical implication of this study was the fact that the observed edge effects increased the dispersion of the uniaxial anisotropy field for the 10×10 mm film by approximately two times. Moreover, the absolute and relative values were obtained for the magnetic properties at the film edges for different target compositions. The obtained results can be readily used by developers and researchers of devices based on thin magnetic films, in particular, sensors for measuring weak magnetic fields [2, 3].

REFERENCES

1. J. Petzold, JMMM, **242**, 84–89 (2002).
2. A. N. Babitskii, B. A. Belyaev, N. M. Boev, *et al.*, Instrum. Exp. Tech., **59**, No. 3, 425–432 (2016).
3. A. N. Babitskii, B. A. Belyaev, N. M. Boev, and A. V. Izotov, in: Proc. IEEE Int. Conf. on Sensors, 1–3 (2017).
4. A. N. Babitskii, B. A. Belyaev, N. M. Boev, A. V. Izotov, and S. A. Kleshnina, Thin-Film Gradiometer, RF Patent No. 26 87557 C1 (2019).
5. B. A. Belyaev, A. V. Izotov, A. A. Leksikov, *et al.*, Izv. Vyssh. Uchebn. Zaved., Fiz., **53**, No. 9/2, 163–165 (2010).
6. B. A. Belyaev, A. A. Leksikov, and A. V. Izotov, Phys. Solid State, **52**, No. 8, 1664–1672 (2010).
7. G. Herzer, JMMM, 157/158, 133–136 (1996).
8. A. V. Izotov, B. A. Belyaev, P. N. Solovev, and N. M. Boev, Physica B Condens. Matter, **556**, 42–47 (2019).
9. B. A. Belyaev, N. M. Boev, A. V. Izotov, and Solovev P. N., Russ. Phys. J., **61**, No. 10, 1798–1805 (2019).
10. B. A. Belyaev, N. M. Boev, A. V. Izotov, *et al.*, Russ. Phys. J., **61**, No. 8, 1367-1375 (2018).
11. B. B. Maranville, R. D. McMichael, S. A. Kim, *et al.*, J. Appl. Phys., **99**, 08C703 (2006).
12. C. E. Murray, J. Appl. Phys., **100**, 103532 (2006).
13. J. Wenisch, C. Gould, L. Ebel, *et al.*, Phys. Rev. Lett., **99**, 077201 (2007).
14. B. A. Belyaev, A. V. Izotov, P. N. Solovev, and N. M. Boev, Phys. Status Solidi R, 1900467 (2019).
15. S. Glathe, M. Zeisberger, R. Mattheis, and D. Hesse, Appl. Phys. Lett., **97**, 112508 (2010).
16. B. A. Belyaev, A. V. Izotov, G. V. Skomorokhov, and P. N. Solovev, Mater. Res. Express, **6**, 116105 (2019).
17. J. A. Thornton, J. Vac. Sci. Technol., **11**, 666–670 (1974).

18. B. A. Belyaev, A. V. Izotov, and P. N. Solovev, Russ. Phys. J., **59**, No. 2, 301-307 (2016).

19. B. A. Belyaev, A. V. Izotov, and A. A. Leksikov, IEEE Sens. J., **5**, 260–267 (2005).

20. B. A. Belyaev, A. V. Izotov, and P. N. Solovev, Physica B Condens. Matter, **481**, 86–90 (2016).

21. B. A. Belyaev, A. V. Izotov, P. N. Solovev, and I. A. Yakovlev, JMMM, **440**, 181–184 (2017).

22. J. Han-Min, C.-O. Kim, T.-D. Lee, and H.-J. Kim, Chin. Phys. Soc., **16**, No. 11, 3520–3535 (2007). DOI: 10.1088/1009-1963/16/11/061

23. K. Hoselitz, Ferromagnetic Properties of Metals and Alloys, Clarendon Press, Oxford (1952).